

# *Structural and hyperfine properties of Mn and Co-incorporated akaganeites*

**Ana E. Tufo, Karen E. García, Cesar A. Barrero & Elsa E. Sileo**

**Hyperfine Interactions**

ISSN 0304-3843

Hyperfine Interact

DOI 10.1007/s10751-013-0830-9



**Your article is protected by copyright and all rights are held exclusively by Springer Science +Business Media Dordrecht. This e-offprint is for personal use only and shall not be self-archived in electronic repositories. If you wish to self-archive your work, please use the accepted author's version for posting to your own website or your institution's repository. You may further deposit the accepted author's version on a funder's repository at a funder's request, provided it is not made publicly available until 12 months after publication.**

## Structural and hyperfine properties of Mn and Co-incorporated akaganeites

Ana E. Tufo · Karen E. García · Cesar A. Barrero ·  
Elsa E. Sileo

© Springer Science+Business Media Dordrecht 2013

**Abstract** The structural and hyperfine properties of pure and substituted akaganeites prepared in the presence of Mn, Co and urea are presented and discussed. In all samples, the chloride content increased with the increase in the urea concentration of the parent solution, and a small Mn-for-Fe or Co-for-Fe substitution occurred. In pure akaganeites, the increase of urea concentration provoked an enlargement of the unit cell volume and a decrease of the crystallinity of the synthesised oxides. The incorporation of Mn and Co provoked changes in cell parameters and an increase in the crystallinity of the samples. The hyperfine parameters for both iron sites of the akaganeites remained practically unchanged, and the spectral areas of the iron sites located close to the chlorides decreased for the doped samples. The recoilless f-factor increased for the substituted akaganeites, indicating an increase in the strength of the atomic bonding of the iron ions.

**Keywords** Akaganeite · Substitution · Mössbauer spectroscopy · X-ray diffraction · Recoilless f-factor

---

Proceedings of the Thirteenth Latin American Conference on the Applications of the Mössbauer Effect, (LACAME 2012), Medellín, Columbia, 11–16 November 2012.

A. E. Tufo · E. E. Sileo (✉)  
INQUIMAE y Facultad de Ciencias Exactas y Naturales, Ciudad Universitaria,  
Pabellón II, Piso 3, CABA, Universidad de Buenos Aires, Buenos Aires, Argentina  
e-mail: sileo@qi.fcen.uba.ar

K. E. García · C. A. Barrero  
Grupo de Estado Sólido, Facultad de Ciencias Exactas y Naturales y Sede de Investigación  
Universitaria, Universidad de Antioquia, Medellín, Colombia

K. E. García  
e-mail: kgarcia05@yahoo.com

## 1 Introduction

Akaganeite ( $\beta$ -FeOOH) is an uncommon mineral in nature, which is mainly found in soils and geothermal brine deposits as an oxidation product of pyrite [1], and as a corrosion product of natural, non-meteoritic minerals [2]. The oxyhydroxide is often detected on iron objects exposed to chloride-containing marine environments [3], and has also been detected as a corrosion product of iron meteorites [4].

Post and Buchwald [5], have studied the crystal structure of the akaganeite formed on an iron meteorite and confirmed that the structure is monoclinic ( $I2/m$ ), and not tetragonal as previously reported by Keller [6]. The solid is formed by four double chains of edge-linked Fe(III)(O,OH)<sub>3</sub> octahedron that shares corners, forming a tunnel hollandite-like (Ba<sub>8</sub>(Mn(IV), Mn(II)<sub>8</sub>O<sub>16</sub>) arrangement, that runs along [010]. The Fe-O octahedron in akaganeite is distorted with Fe-(O,OH) distances ranging from 1.94 to 2.13 Å and shows three longer and three shorter Fe-O distances; as expected the longer distances are associated with the OH<sup>-</sup> anions. Depending on the nature of the precursor, the tunnel is partly occupied by chloride or similar anions such as OH<sup>-</sup> or F<sup>-</sup> [7, 8] that are believed to be essential to maintain the structure. The anions in the tunnel may be exchanged [9]. Post et al. [10] using neutron powder diffraction data have shown that weak hydrogen bonds are formed between the framework O atoms and Cl ions, and that the Cl<sup>-</sup> fills approximately 2/3 of the tunnel sites, suggesting an ordering scheme in a given tunnel with every third tunnel site vacant.

When akaganeite is synthesized in acidic solutions, extra protonated oxide ligands are necessary to balance the Cl anions in the channels or are necessary to balance the charge of substituting lower-valence cations into the octahedral sites. Stahl et al. [11] have proposed that  $\beta$ -FeOOH can be represented by the formula (FeO<sub>1-x</sub>(OH)<sub>1+x</sub>Cl<sub>x</sub>), and showed that the structure did not contain H<sub>2</sub>O molecules.

Akaganeite is an antiferromagnetic material with a Néel temperature of 299 K, and its Mössbauer spectra have attracted a lot of attention because of their complexity in both the paramagnetic and magnetically-ordered states [12]. At the magnetic ordering temperature, the Mössbauer spectra changes from a broad doublet to a sextet, and a careful analysis shows that the broad doublet consists of two doublets rather than just one broadened doublet due to high site distortion. In the magnetically-ordered state, the spectra have an asymmetric appearance, and at least three sextets with differing magnetic hyperfine fields and quadrupole splittings, are needed to fit the spectra. Barrero et al. [13] have found that the two crystallographic sites required by the monoclinic symmetry are only discernible in the low temperature magnetic region. At room temperature, in the paramagnetic state, the spectrum may be fitted with two doublets whose origin is related to the chlorine content, i.e. one doublet is assigned to the Fe(III) ions located close to chloride ions, and the other doublet is assigned to the iron ions located close to chloride vacancy sites. The low temperature magnetic spectra can be adequately fitted with four sextets, whose hyperfine parameters must be subjected to some constraints. The origin of these components is related to the two different crystallographic sites and to the chlorine content. One important parameter which defines the usefulness of the Mössbauer transition is the fraction of gammas which are emitted and absorbed without recoil, i.e. the recoilless  $f$ -fraction [14]. The calculation of the  $f$ -fraction is very important for complete quantitative characterization of a given sample by Mössbauer spectrometry. Among other things, this parameter can be related with the

strength of the atomic bonding, in such a way that at a given temperature a sample with a high  $f$ -fraction could be related with high iron bonding. The  $f$ -fraction also allows the determination of the relative atomic or weight fractions of each iron site in a single phase or of each iron phase present in mixed iron phase [15]. Only few articles have reported  $f$ -fractions of pure akaganeite [15–17] but to the best of our knowledge there are no reports of  $f$  values for doped akaganeites. This work is still to be done.

On the other hand, the substitution of foreign elements in the crystal structure of akaganeite can strongly affect the magnetic hyperfine fields. In natural environments Fe-for-Al substitution is often found because Al is more common in the earth's crust than Fe, and the best documented substitution is that of  $\text{Al}^{3+}$  for  $\text{Fe}^{3+}$ . Cations substitution have been reported for natural and synthetic oxyhydroxides, particularly, goethite [18]. The substitution of Fe(III) for a foreign metal cation usually affects, among others, the unit cell parameters, the chemical reactivity, the crystallinity and the superficial properties of the substituted oxides. If the foreign cation is diamagnetic, the substitution constitutes a strong perturbation of the magnetic properties of Fe oxides, lowering the ordering temperatures and reducing the hyperfine fields at all temperatures. However the magnetic hyperfine fields react similarly to other perturbations: thus small particle size has a similar effect to diamagnetic substitution on the field reduction. Ishikawa et al. [19] have synthesized akaganeite in the presence of Cu(II), Ti(IV), Ni(II), and Cr(III) ions and found that Ti drastically affects the particle size and the crystallite size of akaganeite in comparison to the other cations. A similar result for Ti(IV) was later confirmed [20]. Also the synthesis of  $\beta$ -FeOOH in solutions containing urea and Al(III), Cr(III), and Cu(II) ions (concentration 10 mol%) have been studied by García et al. [21] and the authors reported that the formed akaganeite presented only subtle differences in the crystallographic and hyperfine properties. However when Al(III) (30 mol%) was used, the average crystallite was significantly reduced. The incorporation of Si in akaganeite was studied by Cornell [22] and it was found that the oxyhydroxide incorporated up to 4 mole% Si, and that the presence of Si strongly promoted twinning of akaganeite. The dissolution data indicated that 20 % of the incorporated Si is located on the surfaces of the crystals and the remainder is distributed uniformly in the crystal structure. Akaganeite has been prepared in the presence of manganese with different valence states [9]; the addition of manganese appears to impede crystallization at low pH but improves it at high pH. Holm [23] has synthesized akaganeite in the presence of Cr, Mn, Co, Ni and Zn (50 mol%), and also reported small incorporations of foreign cations.

As a part of a general study about the feasibility of substitution on the structure of akaganeite at different pH values, and in order to determine if the substitution can be derived from Mössbauer spectroscopy measures, we now report the structural and hyperfine characteristics of a series of pure and incorporated akaganeites formed in the presence of Co(II) and Mn(II) ions, and different urea concentrations.

## 2 Materials and methods

Two samples of cobalt doped  $\beta$ -FeOOH were prepared by dissolving in bidistilled water (2000 mL),  $\text{FeCl}_3 \cdot 6\text{H}_2\text{O}$  (53.80 g, 0.198 mol),  $\text{CoCl}_2 \cdot 6\text{H}_2\text{O}$  (5.96 g, 0.025 mol),

and urea  $(\text{NH}_2)_2\text{CO}$  (12.00 or 48.00 g, 0.20 or 0.80 mol). Similarly, two Mn-doped samples were prepared using  $\text{MnCl}_2 \cdot 4\text{H}_2\text{O}$  (3.96 g, 0.016 mol). The four solutions obtained were aged for 48 h at 70 °C in closed polyethylene flasks. The solids were recovered from the suspensions by dialysis through high-purity membranes. The dialysis was carried until the conductivity of the solutions was similar to that of bidistilled water. The suspensions were dried at 40 °C for 48 h. The solids were named as Aka-Co-0.10, Aka-Co-0.40, Aka-Mn-0.10, and Aka-Mn-0.40. Two samples of pure akaganeites were also prepared following the same procedure by dissolving  $\text{FeCl}_3 \cdot 6\text{H}_2\text{O}$  (53.80 g, 0.198 mol), and urea (12.00 or 48.00 g, 0.20 or 0.80 mol) in bidistilled water (final volume 2000 mL). A third sample of pure akaganeite was also prepared, following Cornell and Schwertmann [18], in absence of urea. Samples were named Aka-0.10, Aka-0.40, and Aka-0.

The Fe content in the samples was determined spectrophotometrically using the thioglycolic acid method [24], Mn and Co content was determined by absorption spectrometry, and Cl content was determined by semi-quantitative energy dispersive X-ray analysis (EDS) which was conducted with an Oxford Instruments INCA system. X-ray diffraction patterns were recorded in a Siemens D5000 diffractometer using graphite-monocromated  $\text{Cu K}\alpha$  radiation. The data were analysed using the GSAS [25] system with the EXPGUI interface [26]. The whole X-ray diffraction patterns were used to refine the crystal structures. Starting unit-cell parameters and atomic coordinates for akaganeite were taken from the literature [11], and monoclinic akaganeite was refined using the I2/m group. Peak profiles were fitted using the Thompson-Cox-Hastings pseudo-Voigt function [27]. As powder diffraction patterns show an anisotropic line-shape broadening that is not a smooth function of d-spacing, the mean coherence path dimensions (MCP) or crystallite sizes, were determined in the parallel direction ( $P_{\text{paral}}$ ) and perpendicular direction ( $P_{\text{perp}}$ ) to the anisotropic broadening (002) axis. Crystallite dimensions were calculated making allowances for the instrument broadening function that was previously modelled using NIST SRM 660 lanthanum hexaboride ( $\text{LaB}_6$ ) standard. Preferential orientation was refined using spherical harmonics.  $^{57}\text{Fe}$  Mössbauer spectra were recorded in a conventional Mössbauer spectrometer working in constant acceleration at room temperature. The spectra were analyzed using the MOSF program [28], which is based on non-linear least squares fitting procedures assuming lorentzian Mössbauer lines while the isomer shift value is quoted relative to that of  $\alpha\text{-Fe}$  at 300 K. In order to determine the relative Mössbauer recoilless  $f$ -fractions at room temperature for all akaganeites we prepare two types of absorbers, one of about 15 mg (named sample A) and other of about 20 mg (named sample B), each consisting of homogenous mixtures of the akaganeites and standard natural iron powder. For example, the absorber named as Aka-Co-0.10-Fe-A means that about 15 mg of Aka-Co-0.10 and iron powder were mixed. Similar notation was used for the other samples. The mass of the absorbers was obtained using a microbalance. The absorbers were then carefully placed in a sample holder of 1.26 cm in diameter.

In this work we obtained the recoilless  $f$ -fraction of akaganeite,  $f_{\text{Ak}}$ , relative to that of iron powder,  $f_{\text{Fe}}$ , proceeding similarly as in the work by Oh and Cook [15]. For that purpose we have used the following equation:

$$\frac{f_{\text{Ak}}}{f_{\text{Fe}}} = \left( \frac{m_{\text{Fe}}}{m_{\text{Ak}}} \right) \left( \frac{MW_{\text{Ak}}}{MW_{\text{Fe}}} \right) \left( \frac{A_{\text{Ak}}}{A_{\text{Fe}}} \right) \quad (1)$$

where  $m_{\text{Ak}}$  and  $m_{\text{Fe}}$  stand for the sample masses,  $MW_{\text{Ak}}$  and  $MW_{\text{Fe}}$  are the molar weights, and  $A_{\text{Ak}}$  and  $A_{\text{Fe}}$  are the relative areas of akaganeite and iron powder, respectively.

### 3 Results and discussion

#### 3.1 Chemical analysis

Table 1 shows the nominal preparative and the final concentrations of Co and Mn, expressed as  $\mu_{\text{Me}}$  ratio ( $\mu_{\text{Me}} [\text{mol mol}^{-1} \text{ \%}] = [\text{Me}] \times 100 / [\text{Me}] + [\text{Fe}]$ ; Me: Co or Mn;  $[\text{Me}]$ :  $\text{mol L}^{-1}$ ), in the prepared samples, also the final Cl content, and the initial and final pH values are also shown for all preparations.

From the data reported in Table 1, it is noticed that a major metal incorporation is observed in those samples showing the lower pH values, however in all cases the incorporation is low and in the range 0.05–0.11  $\text{mol mol}^{-1} \text{ \%}$  for Co, and 0.08–0.16  $\text{mol mol}^{-1} \text{ \%}$  for Mn. The low Mn (or Co) for iron substitution in akaganeite may be ascribed to the difference in coprecipitation abilities of the ions with Fe(III) via hydrolysis during the aging. The degree of hydrolysis of the ions can be roughly compared by their first hydrolysis constants, being in the order Fe(III) (pKa: 2.73)  $\gg$  Mn(II) (pKa: 10.46)  $\sim$  Co(II) (pKa: 10.20) [19, 29].

The final Cl content also varied with the urea concentration of the parent solution, and the incorporation increases at higher preparative pH values. The same trend is found in the Co and Mn doped samples. Both the Mn and the Co incorporations are low with values in the range 0.05–0.16, being the incorporation higher in the Mn-doped akaganeites. The foreign metal incorporation decreases with the increase in urea content.

#### 3.2 Structural properties

The results of the Rietveld simulation are presented in Table 2. The XRD diagrams of all samples corresponded to akaganeite. The quality of the refinements was satisfactory and similar for all samples. The profiles of the observed and calculated diffraction patterns and the difference plot for sample Aka-Co-0.40 are shown in Fig. 1. As can be observed, the experimental diagram is well described by the akaganeite structural model that has been employed.

The unit cell volume of pure akaganeites increased from 336.047(23)  $\text{\AA}^3$  to 337.339(34)  $\text{\AA}^3$  with the increase of urea concentration of the preparative solution, and with the increase in Cl content. The calculated crystallite sizes parallel ( $L_{\text{paral}}$ ), and perpendicular ( $L_{\text{perp}}$ ) to the (002) axis of pure akaganeites decrease, from 57 nm to 44 nm for  $L_{\text{paral}}$  and from 140 nm to 117 nm for  $L_{\text{perp}}$ , with the increase of urea content of the parent solution, indicating that the presence of urea decreases the crystallinity of the synthesised oxide.

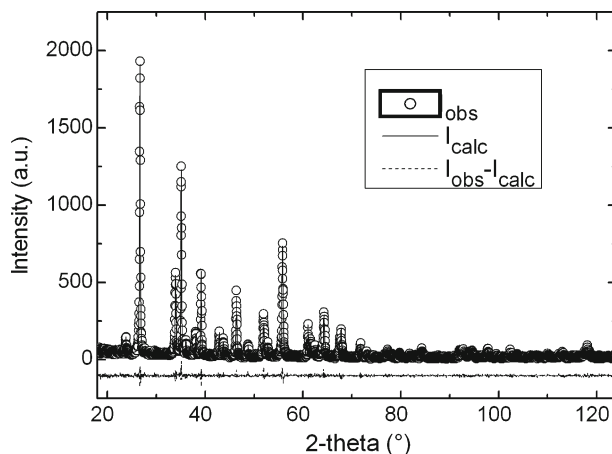
The cell volumes of undoped and Co-doped akaganeites markedly increase with the increment in urea content. However, the opposite trend occurs in the Mn-doped samples, for which the cell volume slightly decreases with increasing urea. Now, for those akaganeites with low urea content, the cell volume slightly increases with Mn (or Co) doping. But, for the samples with high urea content, the opposite behavior

**Table 1** Chemical analysis of the prepared akaganeites

Sample	Aka-0	Aka-0.10	Aka-0.40	Aka-Co0.10	Aka-Co0.40	Aka-Mn0.10	Aka-Mn0.40
$\mu_{Fe}$ [mol mol <sup>-1</sup> %] (nominal)	1	-	-	-	-	-	-
$\mu_{Co}$ [mol mol <sup>-1</sup> %] (nominal)	-	-	-	11.21	11.21	-	-
$\mu_{Mn}$ [mol mol <sup>-1</sup> %] (nominal)	-	-	-	-	-	7.47	7.47
Atomic % (EDS) ratio Fe/Cl	Fe: 25.14 Cl: 3.39 7.42	Fe:24.88 Cl: 3.48 7.15	Fe: 24.49 Cl: 4.25 5.76	Fe: 22.33 Cl: 3.74 5.97	Fe: 27.13 Cl: 5.22 5.20	Fe: 23.73 Cl: 3.46 6.86	Fe: 26.58 Cl: 4.00 6.67
(Atomic %)							
$\mu_{Co}$ [mol mol <sup>-1</sup> %] (incorporated)	-	-	-	0.11	0.05	-	-
$\mu_{Mn}$ [mol mol <sup>-1</sup> %] (incorporated)	-	-	-	-	-	0.16	0.08
Initial and final pH	1.73-1.20	1.74-1.03	1.86-1.42	2.07-1.57	2.17-1.82	2.08-1.54	2.23-1.76



**Fig. 1** Observed and calculated DRX profiles for sample Aka-Co-0.40



is noticed. Therefore, the observed variation in the unit cell parameters can be attributed to concomitant effects coming from the very small Mn (or Co) for Fe substitution, and principally due the variation in the Fe and Cl contents which can be accompanied by the presence of other defects, like more OH- groups, vacancies, etc. Moreover, in this analysis we have to take into consideration the coordination number, the oxidation state and the spin state of the cations, which affects their ionic radii. For example if we assume that Mn and Co are octahedrally coordinated, and that they have 2+ oxidation and high spin states, then the ionic radii for  $\text{Fe}^{3+}$ ,  $\text{Co}^{2+}$ ,  $\text{Mn}^{2+}$  and  $\text{Cl}^{-1}$  should be of 0.645 Å, 0.745 Å, 0.83 Å, and 1.81 Å, respectively [30]. But other radii may occur if other assumptions are considered, which makes the analysis more complex.

The solids obtained in 0.10 M urea showed  $L_{\text{paral}}$  and  $L_{\text{perp}}$  values that changed from 66/118, in pure akaganeite, to 97/108, and to 52/215 in the Co and Mn added samples, indicating that the foreign cation incorporations provoked an increasing elongated form in the domains. In the solids obtained at higher urea concentration (0.40 M) the values changed from 44/117 to 146/40, with the Co incorporation, and to 84/86 with Mn substitution, indicating a marked variation in the form of the domains. These results confirm that crystallinity depend not only on the Me-for-Fe substitution but also on the preparative pH conditions.

### 3.3 Hyperfine properties

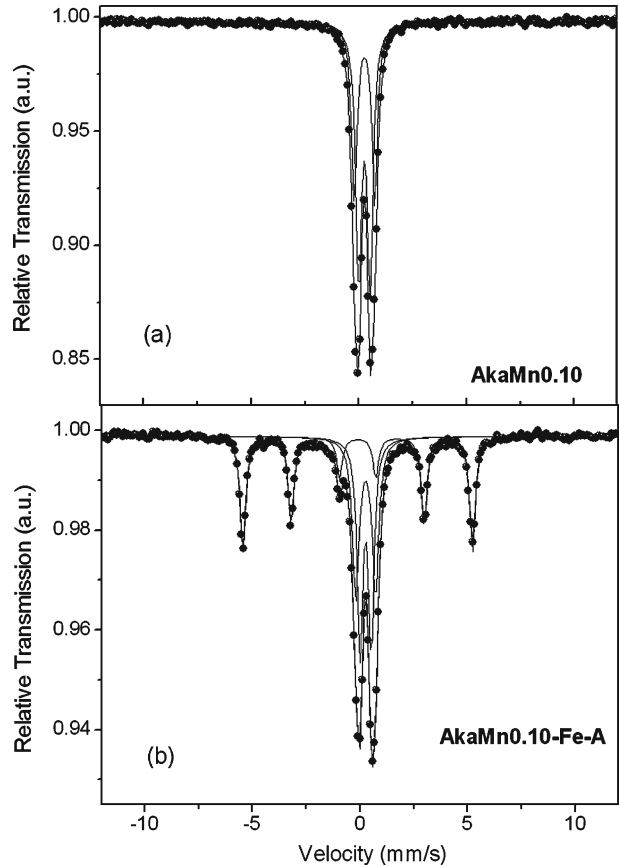
Figure 2a shows the room temperature Mössbauer spectrum of Aka-Mn-0.10. The spectrum was fitted with two components, doublet 1 (D1) and doublet 2 (D2), whose hyperfine parameters are reported in Table 3. Component D1 originates from iron atoms located close to the chloride sites, while component D2 is attributed to iron atoms located close to the chloride vacancy sites. Similar spectra (not shown) were obtained for the other samples. These values are in good agreement with those reported in the literature for pure akaganeites [20]. No signals from other iron phases were detected in good agreement with the XRD findings. Table 3 presents the values of the center shifts,  $\delta$ , the line widths,  $\Gamma$ , and the quadrupole splittings,  $\Delta$ , for both

**Table 2** Structural analysis of the prepared akaganeites

Sample	Aka-0	Aka-0.10	Aka0.40	Aka-Co0.10	Aka-Co0.40	Aka-Mn0.10	Aka-Mn-0.40
$a$ [Å]	10.531(8)	10.534(9)	10.558(9)	10.539(4)	10.544(5)	10.539(8)	10.543(11)
$b$ [Å]	3.031(1)	3.031(1)	3.0328(1)	3.032(1)	3.032(1)	3.0317(1)	3.0309(1)
$c$ [Å]	10.528(5)	10.530(1)	10.534(1)	10.527(1)	10.544(5)	10.544(1)	10.532(8)
$\beta$ [°]	89.99(1)	90.00(1)	89.92(1)	90.03(1)	89.97(1)	89.87(1)	90.00(2)
Volume [Å <sup>3</sup> ]	336.047(23)	336.322(46)	337.339(34)	336.432(22)	337.148(25)	336.797(57)	336.605(35)
$L_{\text{para}}$ [nm]	57	66	44	97	146	52	84
$L_{\text{perp}}$ [nm]	140	118	117	108	40	215	86
R <sub>wp</sub>	8.12	11.88	12.92	14.65	13.02	13.52	13.09
R <sub>p</sub>	6.67	9.58	9.94	10.14	10.25	10.47	7.69
Goff	1.11	1.06	1.09	1.08	1.16	1.16	1.21
R <sub>Bragg</sub>	4.83	10.70	7.62	12.13	9.00	9.80	9.55

**Atomic parameter:**  $z = 0.250$ ; R<sub>p</sub>:  $100 \sum |I_o - I_c| / \sum I_o$ ; R<sub>wp</sub>:  $100 [\sum w_i (I_o - I_c) / \sum w_i I_o]$ ; R<sub>Bragg</sub>:  $100 \sum |I_{k_o} - I_{k_c}| / \sum I_{k_o}$ ; Goff:  $\sum w_i (I_o - I_c) / \sum w_i I_o$ ; I<sub>o</sub> and I<sub>c</sub>: observed and calculated intensities;  $w_i$  weight assigned to each step intensity;  $I_{k_o}$  and  $I_{k_c}$  observed and calculated intensities for Bragg  $k$ -reflection;  $N$  and  $P$  number of data points in the pattern and number of parameters refined. Values in parentheses are esd for the least significant figures of the data shown, the esd values are taken from the final cycle of the Rietveld refinement

**Fig. 2** Room temperature Mössbauer spectra of: **a** Aka-Mn-0.10, and **b** mixture of 9.1 mg of Aka-Mn-0.10 and 5.9 mg of standard iron powder



iron sites in the akaganeites. A comparison between pure and doped samples shows that the values of the parameters remain practically unchanged independently of Co, Mn and urea concentrations. These results suggest that only a very small amount of these cations may have entered into the structure and that the incorporation does not provoke appreciable changes in these hyperfine parameters.

A comparison between the relative area of doublet D1 with the Cl content and also with the Fe/Cl ratio shows an interesting trend for the pure akaganeites (see Tables 1, 2 and 3). The area of D1 behaves similarly as the Fe/Cl ratio, but not similarly with respect to the Cl content, i.e. the area of D1 increase when going from Aka-0, to Aka-0.10, and to Aka-0.40, with the increase of Cl/Fe ratio.

On the other hand, the relative areas of the D1 sites slightly decrease for the doped samples in comparison to those of the pure akaganeites, this effect being more pronounced for Mn-doped than for Co-doped akaganeites.

The small differences between the Fe/Cl ratio of pairs Aka-Co-0.10/Aka-Co-0.40 and Aka-Mn-0.10/Aka-Mn-0.40 are not detected through changes in D1, and the value remains unaltered within each series, presenting values of 61 and 59 for the Co- and Mn-akaganeites, respectively. However, a decrease in the D1 value is observed when samples Aka-0.10, Aka-Co-0.10 and Aka-Mn-0.10 are compared. This change

**Table 3** Hyperfine parameters derived from the fit of the room temperature Mössbauer spectra of the prepared samples

Sample	Component	$\delta$ (mm/s)	$\Gamma$ (mm/s)	$\Delta$ (mm/s)	Area (%)
Aka-0	D1	0.36	0.30	0.54	65
	D2	0.37	0.30	0.97	35
Aka-0.10	D1	0.36	0.28	0.54	63
	D2	0.37	0.30	0.95	37
Aka-0.40	D1	0.36	0.28	0.54	61
	D2	0.37	0.31	0.95	39
Aka-Co-0.10	D1	0.37	0.32	0.53	61
	D2	0.37	0.31	0.95	39
Aka-Co-0.40	D1	0.37	0.31	0.53	61
	D2	0.37	0.30	0.95	39
Aka-Mn-0.10	D1	0.37	0.31	0.52	59
	D2	0.37	0.31	0.95	41
Aka-Mn-0.40	D1	0.37	0.31	0.52	59
	D2	0.37	0.30	0.95	41

Estimated errors are of about  $\pm 0.01$  mm/s for the centre shift,  $\delta$ , line broadening,  $\Gamma$ , and quadrupolar splitting,  $\Delta$ , and of about  $\pm 2$  % for the areas. D1 and D2 stand for doublet 1 and doublet 2, respectively

**Table 4** Masses ( $m_{Ak}$  and  $m_{Fe}$ ) of akaganeite and iron powder used to prepare the absorbers and the relative Mössbauer areas ( $A_{Ak}$  and  $A_{Fe}$ ), for all samples

Sample	$m_{Ak}$ (mg)	$m_{Fe}$ (mg)	$MW_{Ak}$ (g/mol)	$A_{Ak}$	$A_{Fe}$	$f_{Ak}/f_{Fe}$
Aka-0-Fe-A	9.30	5.9	93.59	47.92	52.08	0.98
Aka-0-Fe-B	12.3	7.9	93.59	45.19	54.81	0.89
Aka-Co-0.10-Fe-A	9.1	5.9	95.39	60.27	39.73	1.68
Aka-Co-0.10-Fe-B	12.2	7.8	95.39	58.69	41.31	1.55
Aka-Co-0.40-Fe-A	9.1	5.9	95.93	52.41	47.59	1.23
Aka-Co-0.40-Fe-B	12.2	7.8	95.93	57.77	42.23	1.50
Aka-Mn-0.10-Fe-A	9.1	5.9	93.81	61.71	38.29	1.75
Aka-Mn-0.10-Fe-B	12.2	7.8	93.81	55.98	44.02	1.37
Aka-Mn-0.40-Fe-A	9.1	5.9	94.25	59.34	40.66	1.60
Aka-Mn-0.40-Fe-B	12.2	7.8	94.25	56.67	43.33	1.41

$MW_{Ak}$  molar weight of akaganeite calculated considering the formula of  $\beta\text{-Fe}_{1-y}\text{Me}_y\text{O}_{(1-x)}$  ( $\text{OH})_{1+x}\text{Cl}_x$  and the values reported in Table 1, where Me accounts for Co or Mn

$f_{Ak}/f_{Fe}$  ratio of the recoilless f-factor of akaganeite to that of iron powder, calculated using (1)

$MW_{Fe}$  molar weight of the iron powder (55.845 g/mol)

**Table 5** Average relative recoilless  $f$ -fractions for the akaganeites

Sample	$f_{Ak}/f_{Fe}$
Aka-0	$0.93 \pm 0.06$
Aka-Co-0.10	$1.62 \pm 0.09$
Aka-Co-0.40	$1.36 \pm 0.19$
Aka-Mn-0.10	$1.56 \pm 0.27$
Aka-Mn-0.40	$1.54 \pm 0.13$

may be attributed to the fact that the relative number of the iron ions in the D1 site decreases, because the dopants (Co or Mn ions) prefer to be located at the D1 sites than at the D2 sites, i.e. the dopants prefer to be located at the least distorted sites.

This decrease in the number of Fe atoms in the D1 sites is observed along with an increase in the population of D2 sites, the effect is contrary to that observed with the increase in the Fe/Cl ratio that should indicate a decrease in D2 sites as observed for the pure akaganeites. The decrease in D1 values also may be attributed to variations in the Fe/Cl ratio, however the observed ratio (7.15, 5.97, and 6.86) do not follow the same trend of D1 (63, 61, and 59).

Figure 2b shows the room temperature Mössbauer spectrum of Aka-Mn-0.10-Fe-15. The spectrum was fitted with three components, two doublets (D1 and D2) related to the akaganeite phase and one sextet related to the iron powder. Table 4 list the data related with the calculation of the relative recoilless  $f$ -fractions for all samples.

The averaged relative recoilless  $f$ -fractions ( $f_{\text{Ak}}/f_{\text{Fe}}$ ) calculated using (1), and the errors are reported in Table 5. It is found that within the error bars the  $f_{\text{Ak}}/f_{\text{Fe}}$  values for the the Co- and Mn-akaganeites are relatively similar to each other but markedly increased in comparison to the undoped sample. It is difficult to find a quantitative interpretation for these results because there is no simple relation between the structural, morphological and compositional properties of the samples on the one hand and the observed  $f_{\text{Ak}}/f_{\text{Fe}}$  values on the other hand. We could speculate that the increment in the relative  $f$ -fractions can be related to an increment in the stiffening of the lattice, perhaps due to a strengthening of the atomic bonding of the iron ions in the doped samples. Of course additional measurements are required to support these ideas.

## 4 Conclusions

The hydrolysis of  $\text{FeCl}_3$  solutions at low pH values and in the presence of urea, Co and Mn ions produces impurity-free akaganeites with only small metal for iron substitution in the structure, this incorporation being more effective at the lower urea concentrations.

The urea and the small metal incorporation in the structure induced changes in the Fe to Cl ratio, the form of the crystallographic domains, the relative Mössbauer spectral areas and the relative recoilless  $f$ -fractions. However, within the error bars no changes in the center shift and the line width were observed in the samples. On the other hand, because the quadrupole splittings of the akaganeites were not significantly affected by the presence of urea and Mn or Co, the symmetry of the D1 and D2 sites did not change appreciably.

The present results show that, the properties of akaganeite are slightly affected by Co or Mn at low concentrations. When formed as a corrosion product of weathering, Co- and Mn-doped akaganeite could exhibit very similar properties to that of synthetically pure akaganeite.

**Acknowledgements** This work was supported by the Universidad de Antioquia (Sustainability project of the Solid State Group 2011–2012), COLCIENCIAS (project CO/08/15), and Ministerio de Ciencia y Técnica de Argentina (project PICT 2008–0780)

## References

1. Holm, N.G., Dowler, M.J., Wadsten, T., Arrhenius, G.:  $\beta$ -FeOOH.Cln (akaganéite) and Fe<sub>1-x</sub>O (wüstite) in hot brine from the Atlantis II Deep (Red Sea) and the uptake of amino acids by synthetic  $\beta$ -FeOOH.Cln. *Geochim. Cosmochim. Acta* **47**, 1465–1470 (1983)
2. Holtstam, D.: Akaganéite as a corrosion product of natural, non-meteoritic iron from Oeqertarsuaq, West Greenland GFF **128**, 69–71 (2006)
3. Rémazeilles, C., Refait, P.: On the formation of  $\beta$ -FeOOH (akaganéite) in chloride-containing environments. *Corros. Sci.* **49**, 844–857 (2007)
4. Buchwald, V.F., Clarke Jr., R.S.: Corrosion of Fe-Ni alloys by Cl-containing akaganeite (beta-FeOOH): the Antarctic meteorite case. *Am. Mineral.* **74**, 656–67 (1989)
5. Post, J.E., Buchwald, V.F.: Crystal structure refinement of akaganéite. *Am. Mineral.* **76**, 272–277 (1991)
6. Keller, P.: Eigenschaften von  $(\text{Cl,F,OH})_x\text{Fe}_8(\text{O,OH})_{16}$  und Akaganeite. *Neues Jahrb. Mineral. Abh.* **113**, 29–49 (1970)
7. Dasgupta, D.R., Mackay, A.L.: *J. Phys. Soc. Jpn.* **14**, 932–935 (1959)
8. Mackay, A.L.: *Mineral. Mag.* **32**, 545–557 (1960)
9. Cai, J., Liu, J., Gao, Z., Navrotsky, A., Suib, S.: Synthesis and anion exchange of tunnel structure akaganeite. *Chem. Mater.* **13**, 4595–4602 (2001)
10. Post, J.E., Heaney, P.J., Von Dreele, R.B., Hanson, J.C.: *Am. Mineral.* **88**, 782–788 (2003)
11. Stahl, K., Nielsen, K., Jiang, J., Lebeck, B., Hanson, J.C., Norby, P., van Lanschot, J.: Neutron and temperature resolved synchrotron X-ray powder diffraction study of akaganeite. *Corros. Sci.* **45**, 2563–2575 (2003)
12. Murad, E.: Mössbauer spectroscopy of clays, soils and their mineral constituents. *Clay Miner.* **45**, 413–430 (2010)
13. Barrero, C.A., García, K.E., Morales, A.L., Kodjikian, S., Greneche J.M.: New analysis of the Mössbauer spectra of akaganeite. *J. Phys.: Condens. Matter.* **18**, 6827–6840 (2006)
14. Murad, E., Cashion, J.: Mössbauer spectroscopy of environmental materials and their industrial utilization. Kluwer, Academic Publishers, Boston (2004)
15. Oh, S.J., Cook, D.E.: Mössbauer effect determination of relative recoilless fractions for iron oxides. *J. Appl. Phys.* **85**, 329–332 (1999)
16. De Grave, E., Van Alboom, A.: *Phys. Chem. Miner.* **18**, 337–342 (1991)
17. Vertes, A., Czakó-Nagy, I.: *Electrochim. Acta* **34**, 721–758 (1989)
18. Cornell, R.M., Schwertmann, U.: The iron oxides: structure, properties, reactions, occurrence and uses. Wiley-VCH Verlag GmbH & Co. KGaA, Weinheim (2003)
19. Ishikawa, T., Katoh, R., Yasukawa, A., Kandori, K., Nakayama, T., Yuse, F.: *Corros. Sci.* **43**, 1727–1738 (2001)
20. García, K.E., Morales, A.L., Greneche, J.M., Barrero, C.A.:  $^{57}\text{Fe}$  Mössbauer study of  $\beta$ -FeOOH obtained in presence of  $\text{Al}^{3+}$  and  $\text{Ti}^{4+}$  ions. *Physica B: Condens. Matter.* **389**, 88–93 (2007)
21. García, K.E., Barrero, C.A., Morales, A.L., Greneche, J.M.: Characterization of akaganeite synthesized in presence of  $\text{Al}^{3+}$ ,  $\text{Cr}^{3+}$ , and  $\text{Cu}^{2+}$  ions and urea. *Mater. Chem. Phys.* **112**, 120–126 (2008)
22. Cornell, R.M.: Preparation and Properties of Si Substituted Akaganeite (b-FeOOH). *Zeitschrift für Pflanzenernährung und Bodenkunde. J. Plant. Nutr. Soil Sci.* **155**, 449–453 (1992)
23. Holm, N.G.: Substitution selectivity of some transition elements (Cr, Mn, Co, Ni, Cu, Zn) during formation of  $\beta$ -FeOOH. *GFF Stockholm* **107**, 297–300 (1985)
24. Leussing, D.L., Newman, L.: Spectrophotometric study of the bleaching of ferric thioglycolate. *J. Am. Chem. Soc.* **78**, 552–556 (1956)
25. Larson, A.C., Von Dreele, R.B.: General structure analysis system (GSAS) Los Alamos National Laboratory Report LAUR, pp. 86–748 (1994)
26. Toby, B.H.: EXPGUI, a graphical user interface for GSAS. *J. Appl. Crystallogr.* **34**, 210–213 (2001)
27. Thompson, P., Cox, D.E., Hastings, J.B.: Rietveld refinement of Debye-Scherrer Synchrotron X-ray data from  $\text{Al}_2\text{O}_3$ . *J. Appl. Crystallogr.* **20**, 79–83 (1987)
28. Vandenberghe, R.E., De Grave, E., De Bakker, P.M.A.: On the methodology of the analysis of Mössbauer spectra. *Hyperfine Interact.* **83**, 29–49 (1994)
29. Baes, C.F.J., Mesmer, R.E.: The hydrolysis of cations. Wiley Interscience, New York (1976)
30. <http://abulafia.mt.ic.ac.uk/shannon/ptable.php>. Consulted on Jan. 21, 2013